



Inferring parameters of prey switching in a 1 predator–2 prey plankton system with a linear preference tradeoff



Sofia H. Piltz^{a,b,*}, Lauri Harhanen^a, Mason A. Porter^{c,d,f}, Philip K. Maini^{e,f}

^a Department of Applied Mathematics and Computer Science, Technical University of Denmark, Artillerivej 303B, Kongens Lyngby 2800, Denmark

^b Department of Mathematics, University of Michigan, 2074 East Hall, Ann Arbor, MI 48109–1043, USA

^c Department of Mathematics, University of California, Los Angeles, Los Angeles, CA 90095, USA

^d Oxford Centre for Industrial and Applied Mathematics, Mathematical Institute, University of Oxford, Andrew Wiles Building, Radcliffe Observatory Quarter, Woodstock Road, Oxford OX2 6GG, UK

^e Wolfson Centre for Mathematical Biology, Mathematical Institute, University of Oxford, Andrew Wiles Building, Radcliffe Observatory Quarter, Woodstock Road, Oxford OX2 6GG, UK

^f CABDyN Complexity Centre, University of Oxford, Oxford OX1 1HP, UK

ARTICLE INFO

Article history:

Received 15 December 2017

Revised 29 June 2018

Accepted 6 July 2018

Keywords:

Prey switching

Lotka–Volterra interactions

Linear stability analysis

Planktonic ciliate–algae dynamics

Smoothing out a discontinuous diet switch

PMC–ABC parameter fitting

ABSTRACT

We construct two ordinary-differential-equation models of a predator feeding adaptively on two prey types, and we evaluate the models' ability to fit data on freshwater plankton. We model the predator's switch from one prey to the other in two different ways: (i) smooth switching using a hyperbolic tangent function; and (ii) by incorporating a parameter that changes abruptly across the switching boundary as a system variable that is coupled to the population dynamics. We conduct linear stability analyses, use approximate Bayesian computation (ABC) combined with a population Monte Carlo (PMC) method to fit model parameters, and compare model results quantitatively to data for ciliate predators and their two algal prey groups collected from Lake Constance on the German–Swiss–Austrian border. We show that the two models fit the data well when the smooth transition is steep, supporting the simplifying assumption of a discontinuous prey-switching behavior for this scenario. We thus conclude that prey switching is a possible mechanistic explanation for the observed ciliate–algae dynamics in Lake Constance in spring, but that these data cannot distinguish between the details of prey switching that are encoded in these different models.

© 2018 Elsevier Ltd. All rights reserved.

1. Introduction

Ciliates are eukaryotic single-celled organisms that propel using small protuberances (called *cilia*) that project from their cell body. They feed on small algae and are an important link between the bottom and higher levels of aquatic food webs (Tirok and Gaedke, 2007a). In addition to seasonal variation, ciliates and their algal prey populations vary at shorter-than-seasonal temporal scales. During years when the spring bloom lasts for several weeks (corresponding to approximately 15–30 ciliate generations), algal and ciliate biomasses exhibit recurring patterns of growth followed by decline (Tirok and Gaedke, 2007a). Ciliates have different modes of predatorial behavior, and they can be categorized roughly in terms of more-selective or less-selective feed-

ing habits (Verity, 1991). Some ciliate species can be construed as selective predators, because they hunt as “interception feeders” that scavenge on food particles and intercept them directly. By contrast, “filter-feeder” ciliates sieve suspended food particles and are an example of a less-selective ciliate species. A laboratory experiment on ciliate predator and phytoplankton prey species in Lake Constance reported prey preference and selective feeding in ciliates (Müller and Schlegel, 1999), and it has been suggested that predator–prey interactions between diverse predator and prey plankton communities are the driving force for the sub-seasonal temporal variability observed in ciliate–algal dynamics, especially during periods of the year in which environmental conditions are relatively stable (Tirok and Gaedke, 2010).

In the present paper, we aim to obtain biological insight into the sub-seasonal oscillations in ciliate populations during spring in Lake Constance and more generally into the ecological concept of *prey switching* (Murdoch, 1969), in which predators express a preference (e.g., for more-abundant prey). To do this, we construct

* Corresponding author at: Department of Mathematics, University of Michigan, 2074 East Hall, Ann Arbor, MI 48109–1043, USA.

E-mail address: piltz@umich.edu (S.H. Piltz).

multiple modeling frameworks for a ciliate predator that adaptively changes its diet in response to changes in the abundances of its two prey.¹ Using ciliate–algae interactions in Lake Constance as an example, we focus on adaptive feeding of a predator group between its two different types of prey to investigate both the characteristics of prey switching (specifically, whether it is best described with a steep or a gradual switching function) and whether it is justified to use a reduced modeling framework (specifically, a *piecewise-smooth dynamical system*²) as an approximation of a smooth system.

One can model prey switching with smooth dynamical systems by considering either density-dependent switching (Abrams and Matsuda, 2003) or density-independent switching (Post et al., 2000), or by using information on which prey type was last consumed (van Leeuwen et al., 2013; 2007). By contrast, a piecewise-smooth system arises when one assumes that a switch in a predator's feeding behavior depends on prey abundances. For example, one can posit that a predator behaves as an optimal forager, as its choice to switch prey depends on which diet composition maximizes its rate of energy intake (Boukal and Křivan, 1999; Křivan, 1996; Křivan and Eisner, 2003; 2007; Křivan and Sikder, 1999; Stephens and Krebs, 1987). Using a piecewise-smooth model, it was suggested recently that prey switching gives a possible mechanistic explanation for the dynamics observed in ciliate and algae populations in Lake Constance (Piltz et al., 2014).

In addition to their ecological applications, piecewise-smooth dynamical systems occur in a wide variety of applications (di Bernardo et al., 2008), ranging from mechanical oscillators such as a rocking block (see, e.g., Hogan, 1989) to relay-feedback systems (in which an electrically-operated switch is used to control a process or an electromechanical system (di Bernardo et al., 2001)). Other biological applications include genetic regulatory networks, in which transcription factors either initiate or inhibit the production of proteins after reaching some threshold concentration (Casey et al., 2006; Glass, 1975), and conceptual climate models, in which an abrupt change in a piecewise-smooth system can represent a transition between different regimes in, e.g., large-scale ocean circulation (Stommel, 1961) or the Earth's reflectivity due to ice cover (Abbot et al., 2011). In a finite-dimensional piecewise-smooth dynamical system, the phase space is divided into two or more smooth regions by one or more *switching manifolds* that mark transitions between the regions. For prey switching, each region corresponds to one of a predator's diet choices, so a model that describes the dynamics has a discontinuous right-hand side. Specifically, in this example, the system satisfies a different set of ordinary differential equations (ODEs) in different regions of phase space. In a piecewise-smooth framework, one assumes that a switch from one diet to another occurs instantaneously. Consequently, piecewise-smooth expressions are also used to approximate nonlinear terms, such as sigmoidal or cubic functions, in systems that have sharp transitions between two or more states.

In ecology and numerous other applications, it is important to conduct detailed investigations into different approaches for how to model sharp changes in governing dynamics. On one hand, it is unclear whether there exist “discontinuous predators” who switch their feeding strategy instantaneously, as assumed in a piecewise-smooth model for prey switching. On the other hand, we have not

found evidence for how to distinguish among the possible smooth transition functions that one can choose to model prey switching. By using data on ciliate and algal population dynamics, we illustrate an important example situation in which exploiting different modeling frameworks increases understanding of prey switching and allows one to gain biological insight into it. Consequently, we conclude that it is justified to examine a piecewise-smooth dynamical system, which has fewer parameters than the associated smooth models introduced in this paper, as a simplifying approximation of a smooth dynamical system. We also show that the piecewise-smooth model in Piltz et al. (2014) is both biologically and mathematically consistent as the limit of two smooth systems, which we construct by (i) using a hyperbolic tangent as a transition function from one diet choice to another and (ii) incorporating a parameter that changes abruptly across the discontinuity in the aforementioned model as a system variable with dynamics on a time scale that is comparable to that of the population dynamics of a predator and its two prey. In the second construction, we examine a system with one more dimension than the corresponding piecewise-smooth system.³

The remainder of our paper is organized as follows. In Section 2, we present and briefly discuss the equations for the 1 predator–2 prey piecewise-smooth model from Piltz et al. (2014). This piecewise-smooth dynamical system includes a tilted switching manifold that marks a transition between two smooth parts of phase space. Biologically, these parts represent the predator's adaptive feeding behavior and its two different diet choices: on one side of the switching manifold, the predator's diet consists solely of its preferred prey; on the other side, it consists solely of the alternative prey. We consider two possible regularizations of the model in Sections 2.1 and 2.2, and we derive analytical expressions and carry out linear stability analysis for the coexistence equilibrium (i.e., where all three species coexist at nonzero densities) for each of the two smooth models. We are interested in coexistence steady states because the data that we use include coexistence of predators and multiple prey. In Section 3, we discuss and use these data on adaptively feeding plankton predators to fit model parameters and compare the biomass predictions of our two smooth models. We summarize and discuss similarities and differences between the piecewise-smooth system (analyzed in Piltz et al., 2014) and its two smooth analogs (analyzed in this paper) in Section 4, and we conclude our study in Section 5. We give additional details about our calculations and analysis in a trio of appendices.

³ Mathematically, one can derive different smooth approximations to the same piecewise-smooth system either by “smoothing out” a discontinuity of a piecewise-smooth system using a differentiable transition function of sigmoidal form (Colombo et al., 2012) or by “regularizing” a piecewise-smooth dynamical system (Kuehn, 2015) into a singular perturbation problem (Hinch, 1991; Jones, 1994) that includes multiple time scales by “blowing up” the switching boundary (Sotomayor and Teixeira, 1996; Teixeira and da Silva, 2012). In this work, we do not consider regularizations that include multiple time scales. A subset of us were among the authors of a recent paper (Piltz et al., 2017) on a multiple time-scale system that describes the dynamics of one predator and two prey populations in the presence of rapid evolution of the predator's diet choice. One can also include nonlinear terms when constructing a smooth dynamical system by smoothing out an instantaneous switch using the method developed in Jeffrey (2014, 2016a). These nonlinear terms take into account small effects that are observable only during a switch and vanish for the corresponding piecewise-smooth system (Jeffrey, 2016b). Comparing different smoothed-out or regularized systems both with each other and with an associated piecewise-smooth system is crucial for understanding the relationships between a piecewise-smooth system and its smooth analogs. Relationships between piecewise-smooth systems and the smooth systems that they approximate were investigated from a theoretical point of view in Hogan (2004) and Dankowicz (2007).

¹ Note that “prey switching” in a system of 1 predator and 1 prey refers to a situation in which predation is low at low prey densities but saturates quickly at a large value when the prey is abundant. In such a scenario, one can model the predator–prey interaction using a Holling type-III functional response (Gause et al., 1936; Holling, 1965).

² Piecewise-smooth dynamical systems are a class of discontinuous systems that describe behavior using smooth dynamics of variables, along with abrupt events that change characteristics of the smooth dynamics (di Bernardo et al., 2008; Champneys and di Bernardo, 2008).

2. Methods

We construct two smooth analogs of a piecewise-smooth dynamical system describing a predator population z that can adjust the extent of its consumption of its preferred prey p_1 . When not consuming its preferred prey p_1 , the predator feeds on an alternative prey p_2 . Before introducing our two smooth models (see Sections 2.1 and 2.2), we present the model equations for the piecewise-smooth dynamical system that was developed in Piltz et al. (2014). For each of the three models, we consider standard nonlinearities in the form of Lotka–Volterra predator–prey interactions. Although these nonlinearities are standard, it is convenient for us to use nonstandard notation for the model coefficients that describe them. This notation allows us both to derive the switching condition introduced previously in Piltz et al. (2014) and to compare the two smooth models that we develop in the present paper to this piecewise-smooth system.

We assume that the predator switches to consume only an alternative prey p_2 when it maximizes its fitness by doing so. To describe this situation, Piltz et al. (2014) developed the following piecewise-smooth dynamical system:

$$\dot{x} = \begin{bmatrix} \dot{p}_1 \\ \dot{p}_2 \\ \dot{z} \end{bmatrix} = \begin{cases} f_+ = \begin{bmatrix} (r_1 - \beta_1 z)p_1 \\ r_2 p_2 \\ (eq_1 \beta_1 p_1 - m)z \end{bmatrix}, & \text{if } h = \beta_1 p_1 - a_q \beta_2 p_2 > 0, \\ f_- = \begin{bmatrix} r_1 p_1 \\ (r_2 - \beta_2 z)p_2 \\ (eq_2 \beta_2 p_2 - m)z \end{bmatrix}, & \text{if } h = \beta_1 p_1 - a_q \beta_2 p_2 < 0, \end{cases} \tag{2.1}$$

where r_1 and r_2 (with $r_1 > r_2 > 0$) are the respective per capita growth rates of the preferred and alternative prey, β_1 and β_2 are the respective death rates of the preferred and alternative prey due to attack, $m > 0$ is the predator per capita death rate per day, and $e > 0$ is the predator conversion efficiency. The coefficients q_1 and q_2 are nondimensional parameters that represent the predator’s respective desire to consume the preferred and alternative prey. Thus, the proportion of predation that goes into predator growth is given by eq_1 for the preferred prey and by eq_2 for the alternative prey. In other words, the model in Eq. (2.1) preserves the idea of a predator’s benefit from consuming prey being proportional to predation amount, as is the case in the standard Lotka–Volterra model. Specifically, we consider constant conversion efficiency as a fraction e for each prey, so the benefits from feeding on the preferred and alternative prey are represented by eq_1 and eq_2 , respectively. With $0 \leq q_2 < q_1 \leq 1$, we emphasize the reduced benefit that the predator obtains from the alternative prey compared to its preferred prey. The difference in the benefit is also where the assumed tradeoff lies, as the alternative prey p_2 invests energy in building predator defense mechanisms and is thus a “less edible” prey compared to the preferred prey p_1 , which does not invest energy in predator defense mechanisms. Consequently, we assume that the growth rate of the preferred prey is larger than that of the alternative prey (i.e., $r_1 > r_2$).

To facilitate our comparison between the piecewise-smooth and smooth systems, in our constructions (see Sections 2.1 and 2.2) of two smooth analogs of (2.1), we take $\beta_1 = \beta_2 = 1$ for simplicity. We thereby assume that the predator exhibits adaptive feeding behavior by adjusting its preference (rather than its attack rate) to the governing prey densities. The parameter a_q corresponds mathematically to the slope of the tilted switching manifold, $h = \beta_1 p_1 - a_q \beta_2 p_2 = 0$, between the two vector fields in (2.1). Biologically, a_q is the slope of the assumed linear tradeoff in the predator’s preference for prey. In other words, an increase in specialization towards the preferred prey comes at a cost of predator population growth from feeding on the alternative prey. See

Piltz et al. (2014) for a biological justification of these model assumptions, analysis of the model (2.1), and inferred parameter values for data from Lake Constance.

In the present paper, we construct and carry out linear stability analyses of two novel (to our knowledge) smooth models for an adaptively feeding predator and its two prey. First, in Section 2.1, we formulate an analog of the model in (2.1) as a three-dimensional (3D) smooth dynamical system with hyperbolic tangent functions. Second, in Section 2.2, we construct a four-dimensional (4D) smooth analog of (2.1) by supposing that the desire q_1 to consume the preferred prey changes across the discontinuity in the piecewise-smooth system (2.1). More specifically, we assume that q_1 can change between 1 and 0 as a system variable that is coupled to the population dynamics.

2.1. Smooth model I

We construct a smooth analog (which we call “smooth model I”) of (2.1) using a hyperbolic tangent as a transition function. This yields the following equations of motion:

$$\begin{aligned} \dot{p}_1 &= r_1 p_1 - \beta_1 p_1 z \left(\frac{1 + \tanh(k(\beta_1 p_1 - a_q \beta_2 p_2))}{2} \right) \equiv f(p_1, p_2, z), \\ \dot{p}_2 &= r_2 p_2 - \beta_2 p_2 z \left(\frac{1 - \tanh(k(\beta_1 p_1 - a_q \beta_2 p_2))}{2} \right) \equiv g(p_1, p_2, z), \\ \dot{z} &= eq_1 \beta_1 p_1 z \left(\frac{1 + \tanh(k(\beta_1 p_1 - a_q \beta_2 p_2))}{2} \right) \\ &\quad + eq_2 \beta_2 p_2 z \left(\frac{1 - \tanh(k(\beta_1 p_1 - a_q \beta_2 p_2))}{2} \right) - mz \\ &\equiv l(p_1, p_2, z), \end{aligned} \tag{2.2}$$

where k determines the steepness of the transition function and thus of switches in the predator’s feeding behavior. The dynamical system in Eq. (2.2) incorporates Lotka–Volterra dynamics, and one can construe eq_1 and eq_2 (where $0 \leq q_2 < q_1 \leq 1$), respectively, as one predator’s benefit from eating its preferred and alternative prey. In Section 3.1, we will infer values of k that best fit data from a particular freshwater plankton system. The data were collected in Lake Constance between 1979 and 1999, were presented originally in Tirok and Gaedke (2006, 2007a), and were subsequently analyzed further in several papers (e.g., Tirok and Gaedke, 2007b; Tirok and Gaedke, 2010). See Section 3 for a description of the data.

2.1.1. Linear stability analysis of smooth model I

We are interested in a steady state of (2.2) with $p_1, p_2, z > 0$. We calculate

$$\begin{aligned} f &= p_1 \left(r_1 - z \left(\frac{1 + \tanh(k(p_1 - a_q p_2))}{2} \right) \right) = 0 \\ \Rightarrow z &\left(\frac{1 + \tanh(k(p_1 - a_q p_2))}{2} \right) = r_1 \end{aligned} \tag{2.3}$$

and

$$\begin{aligned} g &= p_2 \left(r_2 - z \left(\frac{1 - \tanh(k(p_1 - a_q p_2))}{2} \right) \right) = 0 \\ \Rightarrow z &\left(\frac{1 - \tanh(k(p_1 - a_q p_2))}{2} \right) = r_2. \end{aligned} \tag{2.4}$$

By setting $\beta_1 = \beta_2 = 1$ and substituting (2.3) and (2.4) into the third equation in (2.2), we obtain

$$\begin{aligned} l &= eq_1 p_1 r_1 + eq_2 p_2 r_2 - mz \\ &= (eq_1 p_1 - m)r_1 + (eq_2 p_2 - m)r_2 = 0. \end{aligned} \tag{2.5}$$

We obtain the steady-state solution $(\tilde{p}_1, \tilde{p}_2, \tilde{z})$, where

$$\begin{aligned} \tilde{z} &= r_1 + r_2, \\ (eq_1\tilde{p}_1 - m)r_1 + (eq_2\tilde{p}_2 - m)r_2 &= 0, \\ \tanh(k(\tilde{p}_1 - a_q\tilde{p}_2)) &= \frac{r_1 - r_2}{r_1 + r_2}. \end{aligned} \tag{2.6}$$

Taking the inverse hyperbolic tangent on both sides of the third equation in (2.6) results in linearly independent equations for \tilde{p}_1 and \tilde{p}_2 . We thereby obtain a unique coexistence steady state at

$$\begin{aligned} \tilde{p}_1 &= \frac{a_q m(r_1 + r_2) + \frac{eq_2 r_2 \operatorname{arctanh}\left(\frac{r_1 - r_2}{r_1 + r_2}\right)}{k}}{e(q_1 a_q r_1 + q_2 r_2)}, \\ \tilde{p}_2 &= \frac{m(r_1 + r_2) - \frac{eq_1 r_1 \operatorname{arctanh}\left(\frac{r_1 - r_2}{r_1 + r_2}\right)}{k}}{e(q_1 a_q r_1 + q_2 r_2)}, \\ \tilde{z} &= r_1 + r_2. \end{aligned} \tag{2.7}$$

All three population densities are positive at the steady state $(\tilde{p}_1, \tilde{p}_2, \tilde{z})$ when

$$k > k_0 = \frac{eq_1 r_1 \operatorname{arctanh}\left(\frac{r_1 - r_2}{r_1 + r_2}\right)}{m(r_1 + r_2)}. \tag{2.8}$$

We use the Routh–Hurwitz criterion (Hurwitz, 1895; Routh, 1877) to investigate the stability of the coexistence steady state (2.7).

Proposition 2.1. *If $a_q \geq q_2/q_1$, then the steady state (2.7) is asymptotically stable if and only if $k > k_0$.*

Proof. See Appendix A. □

Proposition 2.2. *If $a_q < q_2/q_1$, then there exists $k_1 \in (k_0, \infty)$ such that the steady state (2.7) is asymptotically stable if and only if $k \in (k_0, k_1)$.*

Proof. See Appendix A. □

From these results, we see that when a_q is large, which corresponds to a predator with a sharp tradeoff in its prey preference (i.e., a small increase in specialization towards its preferred prey comes at a large cost in growth from feeding on the alternative prey), the coexistence steady state (2.7) is stable for all $k > k_0$. When the prey switching is steep (i.e., when $k \rightarrow \infty$), the coexistence steady state (2.7) is the same as the steady state of the piecewise-smooth system that lies on the switching manifold (the latter steady state is a *pseudoequilibrium*), and it has a complex-conjugate pair of eigenvalues with negative real part when $a_q > q_2/q_1$ (Piltz et al., 2014). However, in contrast to the piecewise-smooth system, in which the coexistence steady state is repelling for shallow or flat prey preference tradeoffs (i.e., when $a_q < q_2/q_1$), the smooth system (2.2) has an interval of intermediate prey-switching slopes $k \in (k_0, k_1)$ (see Eq. (A.9) for the expression for k_1) for which the coexistence state is also stable for $a_q < q_2/q_1$. If $k \notin (k_0, k_1)$, then the coexistence steady state in the smooth system (2.2) is unstable when $a_q < q_2/q_1$.

For population densities at the stable coexistence steady state, smooth model I implies that the predator density is determined solely by the prey growth rates, so it is affected neither by the slope of the tradeoff nor by the steepness of the diet switch (see Eq. (2.7)). For a nearly flat tradeoff (i.e., when a_q is small), the stable coexistence steady-state solution for the preferred prey p_1 is at its minimum. (See, e.g., the parameter values in the caption of Fig. 1.) However, if in addition to a mild tradeoff, the predator's prey switching is also gradual (i.e., k is very small), then p_1 is large at the stable equilibrium (see the left panel of Fig. 1). This pattern of minimum and maximum values is the reverse for the alternative prey: The steady-state concentration of the alternative prey p_2 has a large value when a_q is small, except for very small k , when the steady-state value of p_2 is small (see the right panel of Fig. 1). Such

behavior of the steady state (2.6) suggests that $k \rightarrow 0$ is a singular limit of smooth system I (2.2).

2.2. Smooth model II

As an alternative to the 3D smooth dynamical system with hyperbolic tangent functions that we formulated in Section 2.1, we now construct a 4D smooth analog of (2.1) by supposing that the predator's desire q_1 to consume the preferred prey is a system variable q that changes along with the population dynamics. To smooth out the 3D piecewise-smooth system (2.1) into a 4D smooth system, we construct expressions for the temporal evolution of the predator's trait to accompany the population dynamics of the predator and the two prey. Biologically, we are assuming that the predator's desire to consume its preferred prey undergoes either *rapid evolution* (Fussmann et al., 2007) or *phenotypic plasticity* (Kelly et al., 2012), which are the two main forms of adaptivity in organisms. We will comment on these model assumptions in Section 4. We thereby turn the parameter q_1 , which changes abruptly across the discontinuity in the piecewise-smooth model (2.1) (i.e., $q_1 = 1$ when $h > 0$ and $q_1 = 0$ when $h < 0$), into a system variable q that changes in response to prey abundance on the same time scale as the population dynamics in a smooth dynamical system.

To ensure similarity with the piecewise-smooth model (2.1), we assume that no preference towards the preferred prey amounts to a feeding mode of consuming only the alternative prey (i.e., $q = 0$) and that maximum preference towards the preferred prey amounts to a feeding mode of consuming only the preferred prey (i.e., $q = 1$). We incorporate this assumption with a bounding function $q(1 - q)$ in the expression for the temporal evolution of the predator's trait. From the condition for prey switching that we derived using optimal-foraging theory (Stephens and Krebs, 1987) in Piltz et al. (2014), we impose that the rate of change of the mean trait value is proportional to $p_1 - a_q p_2$. That is, we assume that the predator's choice to switch prey depends on prey abundances and which diet composition maximizes its rate of energy intake (Stephens and Krebs, 1987). For simplicity, we also assume exponential prey growth and a linear functional response, as in the piecewise-smooth system (2.1) (Piltz et al., 2014). We thereby obtain the following dynamical system for the population dynamics coupled with temporal evolution of the predator trait:

$$\begin{aligned} \frac{dp_1}{dt} &= g_1(p_1, p_2, z, q) = r_1 p_1 - q p_1 z, \\ \frac{dp_2}{dt} &= g_2(p_1, p_2, z, q) = r_2 p_2 - (1 - q) p_2 z, \\ \frac{dz}{dt} &= g_3(p_1, p_2, z, q) = eq p_1 z + e(1 - q) q_2 p_2 z - mz, \\ \frac{dq}{dt} &= f(p_1, p_2, q) = q(1 - q)(p_1 - a_q p_2). \end{aligned} \tag{2.9}$$

As with the piecewise-smooth system (2.1) and smooth system I (2.2), the predator–prey interaction in (2.9) (which we call “smooth model II”) is of standard Lotka–Volterra type, so the benefit of consuming prey is proportional to the amount of predation. Consequently, the proportion of predation that goes into predator growth is given by eq for the preferred prey and by $e(1 - q)q_2$ for the alternative prey, where $e \in (0, 1)$ is a parameter that represents conversion efficiency. For $q_1 = 1$ in the piecewise-smooth system (2.1), smooth model II (2.9) reduces to f_+ in (2.1) when $q = 1$ and to f_- in (2.1) when $q = 0$. Biologically, these two cases correspond, respectively, to the situations in which the predator's diet is composed solely of the preferred prey and solely of the alternative prey. Note that the model in (2.9) does not include a time-scale difference, which we incorporated between demographic and trait

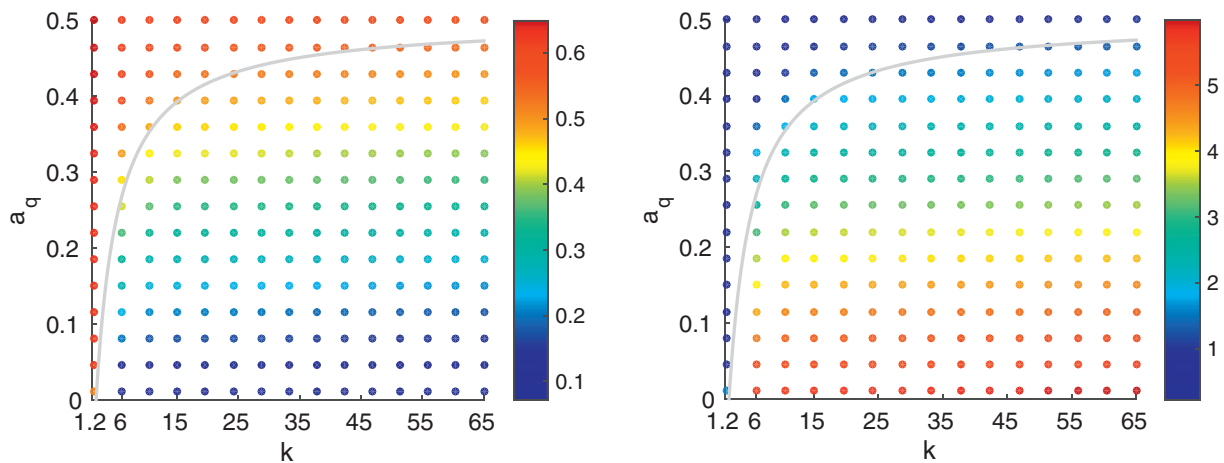


Fig. 1. Numerical computations for prey population densities at the steady state in Eq. (2.7) for the parameter values $(e, \beta_1, \beta_2, r_1, r_2, m, q_1, q_2) = (0.25, 1, 1, 1.3, 0.26, 0.14, 1, 0.5)$ (where we determine the values of r_1, r_2 , and m from our parameter fitting of the piecewise-smooth model in Piltz et al., 2014) of (left) the preferred prey p_1 and (right) the alternative prey p_2 at the indicated values of the slope a_q of the preference tradeoff (vertical axis) and steepness k of the predator switching (horizontal axis). The predator population density at steady state is $\bar{z} = r_1 + r_2 \approx 1.56$. We indicate the value of the prey density at steady state in color and numerically compute the steady-state solution of smooth system I (2.7). The steady state is stable above the gray curve. (See the equation for k_1 in Eq. (A.9).) With these parameter values, k_0 in Eq. (2.8) is approximately 1.197.

(i.e., q_1) dynamics in a similar 4D smooth system and analyzed using singular perturbation theory in Piltz et al. (2017).

2.3. Linear stability analysis of smooth model II

The population densities of the two prey and the predator at the coexistence steady state in smooth system II (2.9) are given by $(\tilde{p}_1, \tilde{p}_2, \tilde{z})$, with

$$\begin{aligned} \tilde{p}_1 &= \frac{a_q m (r_1 + r_2)}{e(r_1 a_q + r_2 q_2)}, \\ \tilde{p}_2 &= \frac{m(r_1 + r_2)}{e(r_1 a_q + r_2 q_2)}, \\ \tilde{z} &= r_1 + r_2, \\ \tilde{q} &= \frac{r_1}{r_1 + r_2}. \end{aligned} \quad (2.10)$$

The same densities occur both for the coexistence steady state of smooth system I (2.7) with steep prey switching (i.e., when $k \rightarrow \infty$) and at the pseudoequilibrium point of the piecewise-smooth system (2.1) (for $q_1 = 1$) that is located on the discontinuity boundary of the piecewise-smooth 1 predator–2 prey model (Piltz et al., 2014).

We summarize the results of linear stability analysis of smooth system II (2.9) in the following two propositions.

Proposition 2.3. *If $a_q = q_2$, then all eigenvalues of the steady-state solution are purely imaginary.*

Proof. See Appendix B. \square

Proposition 2.4. *If $a_q \neq q_2$, then the steady state is linearly unstable.*

Proof. See Appendix B. \square

Consequently, smooth system II (2.9) has an unstable coexistence steady state irrespective of whether one can construe a predator as selective with a sharp preference tradeoff with respect to its preferred and alternate prey or as unselective with a mild tradeoff in its preference towards the two prey. Our results also imply that our smoothing of the piecewise-smooth system (2.1) by adding an extra dimension as in Eq. (2.9) changes the stability of the coexistence steady state.

3. Results

To obtain insight into the steepness of the prey switching in the two smooth models that we constructed in Section 2, we consider data from Lake Constance (see Tirok and Gaedke, 2006; Tirok and Gaedke, 2007b) for ciliate predators and two different types of their algal prey groups. The Lake Constance data set consists of over 23,000 observations of abundances (expressed either as individuals or as cells per milliliter) and biomass (expressed as units of carbon per square meter) of various plankton species obtained at least once in a sample of a few milliliters to a liter of water between March 1979 and December 1999. We compare the abundances predicted by our two smooth models with data from years 1991 and 1998. (For a comparison between the piecewise-smooth model (2.1) and data, see Piltz et al., 2014.) During these two years, the spring bloom lasted for several weeks (Tirok and Gaedke, 2006; 2007b).

In Lake Constance, ciliates coexist with their algal prey for several generations (and at a high biomass) during years when the spring bloom occurs under mildly variable environmental conditions (Tirok and Gaedke, 2007a). Additionally, the ciliate and algal biomasses exhibited recurring patterns (which are often interpreted as a result of predator–prey interactions) of increases followed by declines in the years 1991 and 1998 (Tirok and Gaedke, 2007a). We are interested in spring abundances, because previous studies have suggested that predator–prey feeding interactions are an important factor in explaining the ciliate–algae dynamics in that season (Tirok and Gaedke, 2010). Thus, during these years, our principal model assumptions (e.g., we do not include fluctuating environmental conditions) are more likely to hold than during other years in the Lake Constance data set. Moreover, previous studies have shown that predator–prey interactions are more important than environmental conditions, especially during spring, for explaining the ciliate–algae dynamics (Sommer et al., 2012). We therefore choose the spring period in these two years for our comparison between model simulations and data.

Müller and Schlegel observed that ciliates actively select against certain types of prey when offered a mixed diet of different types of their algal prey (Müller and Schlegel, 1999). They suggested that adaptive feeding in ciliates occurs because different species benefit differently in a way that depends on the match between their feeding mode and the species that are abundant in the prey

community. That is, ciliates select against their less-edible prey (e.g., a prey type that develops a hard silicate cover as a predator defense mechanism) when offered a mixed diet of both easily-digested and less-edible prey (Müller and Schlegel, 1999). As a representative of an easily-digested prey group (i.e., the preferred prey p_1 in our models), we consider data for *Cryptomonas ovata*, *Cryptomonas marssonii*, *Cryptomonas reflexa*, *Cryptomonas erosa*, *Rhodomonas lens*, and *Rhodomonas minuta* in the Lake Constance data set. For the less-edible prey (i.e., the alternative prey group p_2), we use data for small and medium-sized *Chlamydomonas* spp. and *Stephanodiscus parvus*. In addition to different prey groups, one can categorize ciliate predators, which dominate the herbivorous zooplankton community in spring (Tirok and Gaedke, 2007a), roughly in terms of being more-selective or less-selective predators (Verity, 1991). To represent differences in selectivity between different predator species, our unselective filter-feeder predator group consists of data for *Rimostrombidum lacustris*, and our selective interception-feeder predator group consists of data for *Balanion planctonicum*.

We use the Lake Constance data on ciliate predators and their algal prey to infer the steepness k of the prey-switching function in smooth model I (2.2); a perturbation parameter (which we denote by ν and discuss in Sections 3.2) in the predator population that measures its departure from the coexistence steady state (2.10) of smooth model II (2.9); and the prey growth, predator death rates, and other parameters of our models. For our comparison between the Lake Constance data and the two smooth models in Sections 3.1 and 3.2, we first normalize both the data points and the model predictions for the predator density z by their L_2 norm (i.e., by Euclidean distance). We consider the time window from 1 March to 15 June, for which there are 31 data points for the selective predator and 19 data points for the unselective predator in 1991. In 1998, there are 15 data points for both the selective and unselective predator species between 1 March and 15 June. We fit parameters to data with approximate Bayesian computation (ABC) combined with a population Monte Carlo (PMC) method (Beaumont et al., 2009). This combination allows us to study the results from the posterior parameter distribution, rather than just from a single value that gives the best fit as a result of an optimization method. The posterior parameter distribution, which is an output of the fitting algorithm, is especially useful for assessing how well the piecewise-smooth model (2.1) approximates prey switching, which we represent with a hyperbolic tangent function in smooth model I (2.2) and by incorporating an additional system variable in smooth model II (2.9).

3.1. Comparison of simulations of smooth model I with Lake Constance data

We compare our simulations of smooth model I with Lake Constance data on selective and unselective predator groups, and we report the results of our parameter fitting for the selective and unselective predator groups using the PMC-ABC method (Beaumont et al., 2009). See Fig. 2 for our results for 1991 and Fig. 3 for our results for 1998. In our comparison, we use fitted values for the growth rates (r_1 and r_2 , respectively) of the preferred and alternative prey, the predator mortality rate m , the slope k of the prey-switching function, and the slope a_q of the prey-preference tradeoff of smooth model I (2.2). Additionally, we use a_q as a bifurcation parameter. (See Propositions 2.1 and 2.2.) However, for simplicity (and similar to the study of the piecewise-smooth system in Piltz et al., 2014), we assume that the nondimensional preference parameters are fixed (and we take $q_1 = 1$ and $q_2 = 0.5$). Thus, given our choice of the preference parameters and using a_q as a bifurcation parameter, we investigate linear preference trade-

offs that all go through point $(q_1, q_2) = (1, 0.5)$, but they do so with different slopes.

Smooth model I (2.2) reproduces the peak abundances in the Lake Constance data and yields an oscillatory pattern for both the selective and unselective predator populations during the springs of 1991 and 1998 (see Figs. 2 and 3, respectively). Additionally, our parameter fitting suggests that adaptive feeding of the selective predator is best represented with a steep switching function. In particular, for 1998, we obtain gradual prey-switching functions for an unselective predator more frequently than we do for a selective one at the smallest tolerance level of the fitting algorithm.⁴ See the center rows of Figs. 2 and 3. Note that the coexistence steady state is unstable for the inferred parameter values that we use in the top-right panels in Figs. 2 and 3. In these two figures, this steady state is thus unstable for $k > k_1 \approx 1.3$ and $k > k_2 \approx 2.9$, respectively (see also Fig. 1).

3.2. Comparison of simulations of smooth model II with Lake Constance data

To compare simulations of the smooth model (2.9) to data, we use the fitted prey growth rates r_1 and r_2 , the predator mortality rate m , and a perturbation parameter ν that measures the departure of the predator population from the coexistence steady state (2.10) for $a_q = a_2 = 0.5$ (so that all four eigenvalues of the coexistence steady state are purely imaginary). We thus use $(p_1(0), p_2(0), z(0), q(0)) = (a_q m(r_1 + r_2) / [e(r_1 a_q + r_2 q_2)], m(r_1 + r_2) / [e(r_1 a_q + r_2 q_2)], \nu(r_1 + r_2), r_1 / (r_1 + r_2))$ as our initial value for the model simulations to infer values for ν that minimize the distance in Eq. (C.1) between the data points and the model for these points. Thus, a small perturbation ν suggests a gradual diet change and that q oscillates around its steady-state value, whereas one can interpret a large perturbation ν from the steady state as a rapid change in the diet (and the dynamics of q).

Smooth model II (just like smooth model I) reproduces the peak predator densities, and it seems that smooth model II best fits the data when there is a large perturbation from the coexistence steady state. See Figs. 4 and 5. For the year 1991, we find that the selective predator group switches its diet less frequently than the unselective predator. Additionally, $q(t)$ reaches its maximum value (of 1) and minimum value (of 0). By contrast, for the unselective predator, there is a change from decreasing $q(t)$ to increasing $q(t)$ at some intermediate value (and not only after reaching the minimum value of 0). See the dynamics of $q(t)$ in the bottom portions of the top panels of Figs. 4 and 5. We find (see Fig. 5) that the switching (with $q(t)$ alternating between 0 and 1) of the selective predator occurs more often in year 1998 than in year 1991. In 1998, we also find that the selective predator switches more often than the unselective predator. In 1991, however, the selective predator switches less often than the unselective predator.

To evaluate how well smooth model II (2.9) predicts prey abundance data (to which it was not fitted), we simulate it with parameter values that we obtain by fitting the model to the unselective predator in year 1991. Our model output for prey abundances suggests for an unselective predator in year 1991 that the preferred prey has smaller-amplitude oscillations than the alternative prey. As we show in Fig. 6, this differs qualitatively from the data. We obtain the same result for smooth model I (2.2) (comparison not

⁴ Using Bayesian estimation (BEST) (Kruschke, 2013) to compare the posterior distributions for the selective and unselective predator groups, we find that the mode of the difference of the k values is 30 and that the 95% highest posterior density interval (HDPI) (i.e., the total mass of points inside the 95% HDPI constitutes 95% of the distribution) is from 5 to 45. Because 0 is not part of this interval, we conclude that our parameter fitting implies that one can model the selective predator group with a credibly larger k than for the unselective predator group.

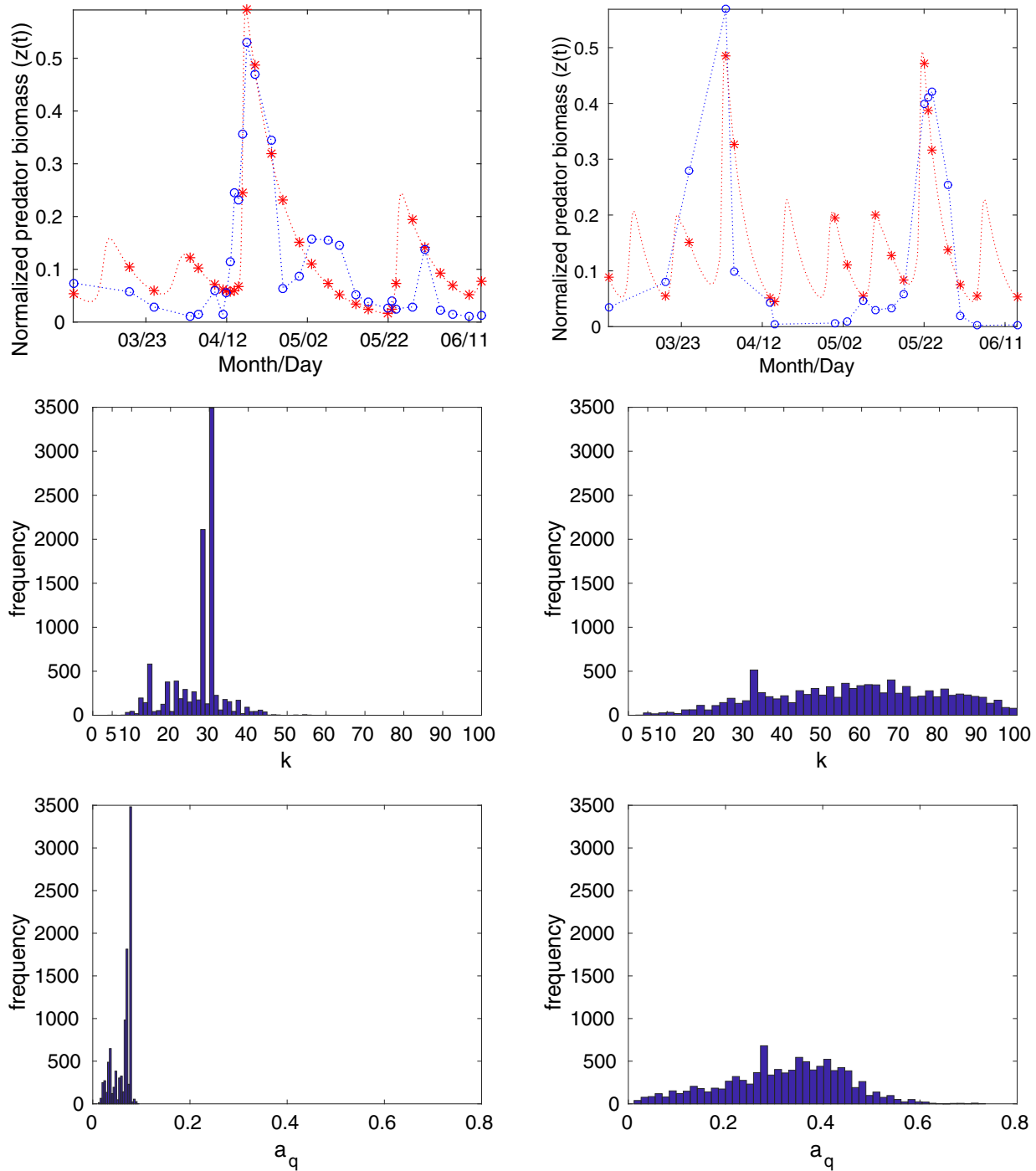


Fig. 2. Comparison of smooth model I and 1991 Lake Constance data for (left) selective and (right) unselective predators. (Top panels) The red asterisks give the normalized predator abundance $z(t)$ for simulations of smooth model I (2.2), and the blue circles give the normalized data for the (left) selective and (right) unselective predator groups in spring in Lake Constance in 1991. We show bar plots for the frequency of (center panels) k values and (bottom panels) a_q values at the strictest tolerance level using the PMC-ABC method (Beaumont et al., 2009). We simulate the model using the parameter values $q_1 = 1$, $q_2 = 0.5$, $e = 0.25$, and $\beta_1 = \beta_2 = 1$ and fitted values of (left) $r_1 \approx 1.64$, $r_2 \approx 0.62$, $m \approx 0.11$, $a_q \approx 0.02$, and $k \approx 31$ and (right) $r_1 \approx 2.54$, $r_2 \approx 0.61$, $m \approx 0.21$, $a_q \approx 0.04$, and $k \approx 67$. For the fitted parameter values, we use (left) the maximum likelihood estimate and (right) the estimate in the posterior distribution that yield the minimum distance between the model and the data. To guide the eye, we show simulation results in red between the asterisks and we plot blue lines between the data points. Each frequency plot (center and bottom panels) represents a random weighted sample (of size 10,000) from the PMC-ABC's posterior distribution of the parameter values accepted at the strictest tolerance level (i.e., $\text{Tol}_{10} \approx 0.00789$ in the left panels and $\text{Tol}_{15} \approx 0.0258$ in the right panels). (We use MATLAB's (The MathWorks, Inc., 2014) 'randsample' function to produce the random sample.) The squared distances (see Eq. (C.1)) between the asterisks (model) and circles (data) are (left) 0.0094 and (right) 0.0102. For more details on parameter fitting, see Appendix C. The unselective predator group consists of data for *Rimostrombidum lacustris*, and the selective predator group consists of data for *Balanion planctonicum*. (To interpret the references to color in this figure legend, see the electronic version of this article.)

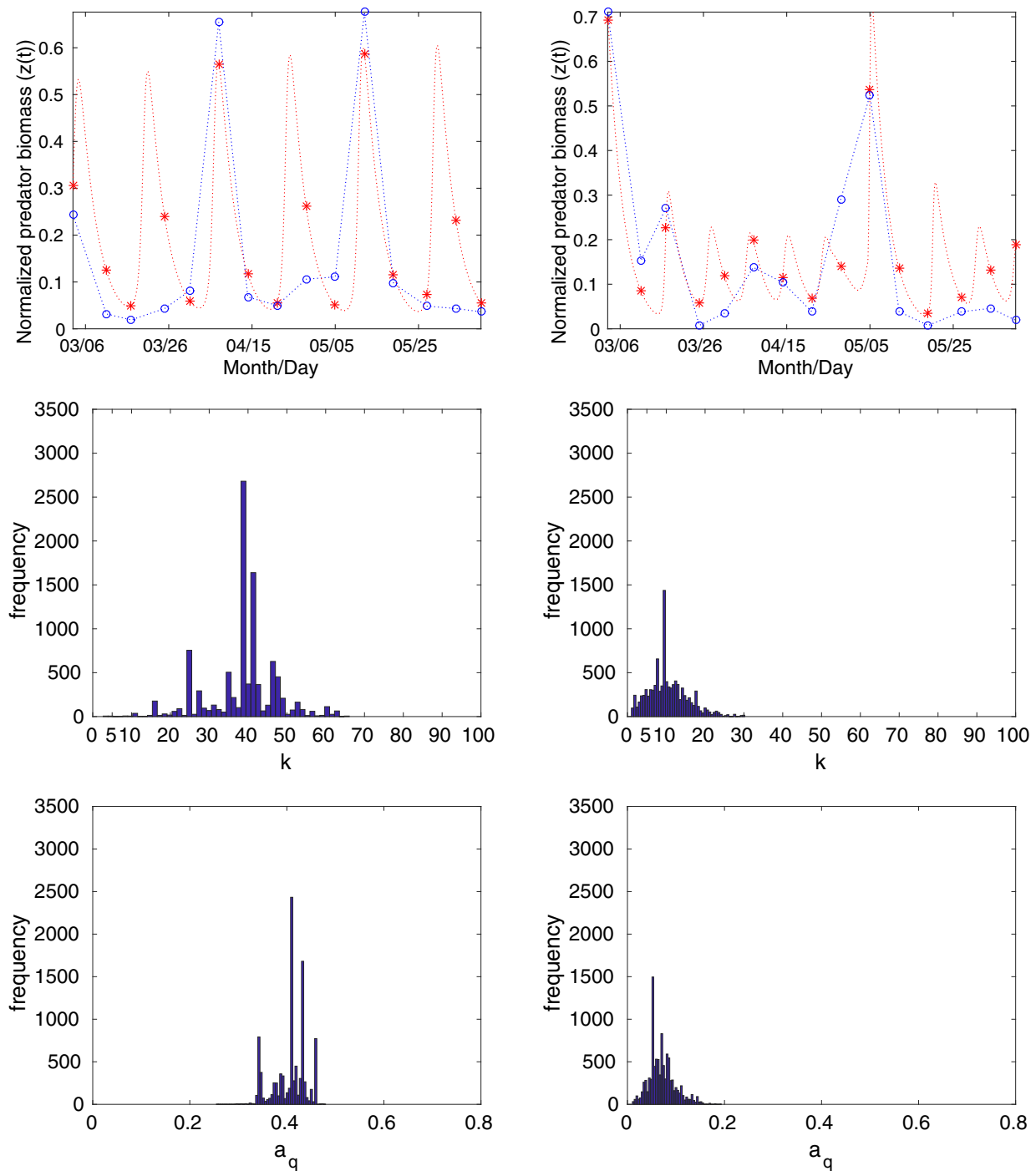


Fig. 3. Comparison of smooth model I and 1998 Lake Constance data for (left) selective and (right) unselective predators. (Top panels) The red asterisks give the normalized predator abundance $z(t)$ for simulations of smooth model I (2.2), and the blue circles give the normalized data for the (left) selective and (right) unselective predator groups in spring in Lake Constance in 1998. We show bar plots for the frequency of (center panels) k values and (bottom panels) a_q values at the strictest tolerance level using the PMC-ABC method (Beaumont et al., 2009). We simulate the model using the parameter values $e = 0.25$ and $\beta_1 = \beta_2 = 1$ and fitted values of (left) $r_1 \approx 1.12$, $r_2 \approx 0.76$, $m \approx 0.25$, $a_q \approx 0.42$, and $k \approx 38$ and (right) $r_1 \approx 2.32$, $r_2 \approx 0.51$, $m \approx 0.27$, $a_q \approx 0.027$, and $k \approx 16$. For the fitted parameter values, we use those in the posterior distribution that yield the minimum distance between the model and the data. To guide the eye, we show simulation results in red between the asterisks and we plot blue lines between the data points. Each frequency plot (center and bottom panels) represents a random weighted sample (of size 10,000) from the PMC-ABC's posterior distribution of the parameter values accepted at the strictest tolerance level (i.e., $\text{Tol}_{15} \approx 0.0213$ in the left panels and $\text{Tol}_{15} \approx 0.0229$ in the right panels). The squared distances (see Eq. (C.1)) between the asterisks (model) and circles (data) are (left) 0.0090 and (right) 0.0061. For more details on parameter fitting, see Appendix C. The unselective predator group consists of data for *Rimostrombidum lacustris*, and the selective predator group consists of data for *Balanion planctonicum*. (To interpret the references to color in this figure legend, see the electronic version of this article.)

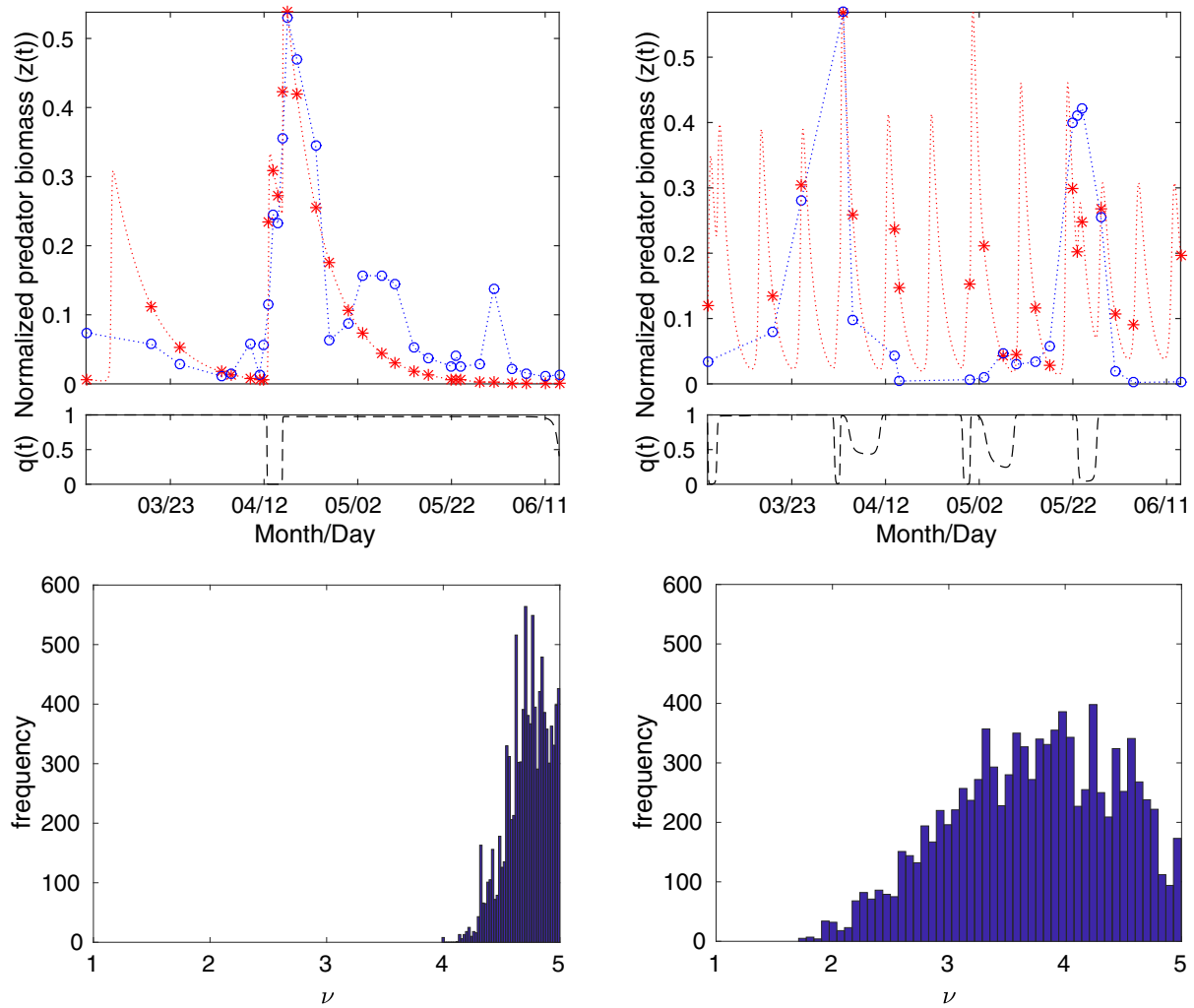


Fig. 4. Comparison of smooth model II and 1991 Lake Constance data for (left) selective and (right) unselective predators. (Top panels) The red asterisks give the normalized predator abundance $z(t)$ for simulations of smooth model II (2.9), and the blue circles give the normalized data for the (left) selective and (right) unselective predator groups in spring in Lake Constance in 1991. (Bottom panels) We show bar plots for the frequency of ν values at the strictest tolerance level using the PMC-ABC method (Beaumont et al., 2009). We simulate the model with an initial value of $z(0) = \nu(r_1 + r_2)$ (where the parameter ν indicates the perturbation of the predator population from the coexistence steady state); the steady-state densities in (2.10); parameter values of $e = 0.25$, $\beta_1 = \beta_2 = 1$, and $a_q = q_2 = 0.5$; and fitted values of (left) $r_1 \approx 3.00$, $r_2 \approx 0.62$, $m \approx 0.12$, and $\nu \approx 4.8$ and (right) $r_1 \approx 2.21$, $r_2 \approx 0.33$, $m \approx 0.48$, and $\nu \approx 4.6$. For the fitted parameter values, we use those in the posterior distribution that yield the minimum distance between the model and the data. To guide the eye, we show simulation results in red between the asterisks and we plot blue lines between the data points. Each frequency plot (bottom panels) represents a random weighted sample (of size 10,000) from the PMC-ABC's posterior distribution of the parameter values at the strictest tolerance level (i.e., $\text{Tol}_{10} \approx 0.00815$ in the left panel and $\text{Tol}_{13} \approx 0.0233$ in the right panel). The squared distances (see Eq. (C.1)) between the asterisks (model) and circles (data) are (left) 0.0038 and (right) 0.0151. For more details on parameter fitting, see Appendix C. The unselective predator group consists of data for *Rimostrombidum lacustris*, and the selective predator group consists of data for *Balanion planctonicum*. (To interpret the references to color in this figure legend, see the electronic version of this article.)

shown). Nevertheless, although we only use predator data to fit parameters, smooth model II (2.9) is able to successfully capture some features of the prey data. As we illustrate in the left panel of Fig. 6, these features include the periodicity of the peak densities of the preferred prey populations.

4. Discussion

From a biological perspective, using a smooth dynamical system allows us to relax the assumption of a “discontinuous” predator of the piecewise-smooth system (2.1). When the discontinuity is smoothed out using hyperbolic tangent functions, as in smooth model I (2.2), we can use data to determine the steepness of the transition in the predator's feeding behavior for a particular predator type. Indeed, our parameter fitting to Lake Constance data suggests that one can model prey switching of either selective or unselective predator species with a steep hyperbolic tangent function.

Additionally, our parameter fitting of smooth model I (2.2) indicates that the best fit to the data occurs in the parameter regime in which the coexistence steady state is unstable. Additionally, simulations of smooth model II (2.9), which smooths out the abrupt change in the predator's diet choice by considering a predator trait as a system variable, exhibits rapid predator-trait dynamics (i.e., the temporal evolution of the predator's desire to consume the preferred prey p_1), suggesting that the best fit to data occurs when the change of diet is abrupt.

From a modeling perspective, the piecewise-smooth system (2.1) incorporates the effects of a predator's adaptive change of diet in response to prey abundance, whereas smooth system II (2.9) (with an appropriate choice of parameter values) explores rapid evolutionary change in a predator's desire to consume its preferred prey (Piltz et al., 2017). Consequently, smooth system II models a different mechanism (namely, *rapid evolution*; Fussmann et al., 2007) than the piecewise-smooth system (which

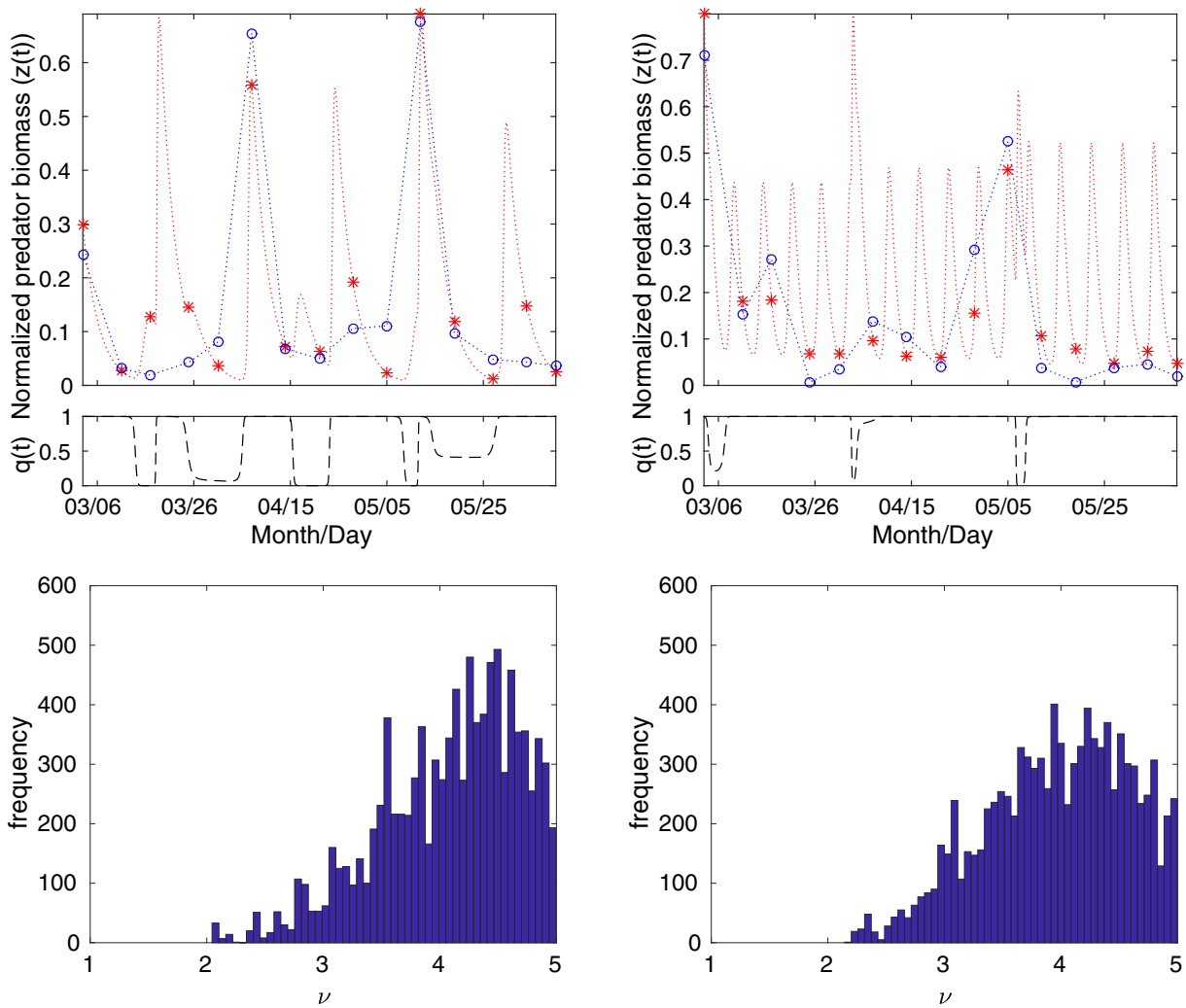


Fig. 5. Comparison of smooth model II and 1998 Lake Constance data for (left) selective and (right) unselective predators. (Top panels) The red asterisks give the normalized predator abundance $z(t)$ for simulations of smooth model II (2.9), and the blue circles give the normalized data for the (left) selective and (right) unselective predator groups in spring in Lake Constance in 1998. (Bottom panels) We show bar plots for the frequency of ν values at the strictest tolerance level using the PMC-ABC method (Beaumont et al., 2009). We simulate the model with an initial value of $z(0) = \nu(r_1 + r_2)$ (where the parameter ν indicates the perturbation of the predator population from the coexistence steady state); the steady-state densities in (2.10); parameter values of $e = 0.25$, $\beta_1 = \beta_2 = 1$, and $a_q = q_2 = 0.5$; and fitted values of (left) $r_1 \approx 1.62$, $r_2 \approx 0.40$, $m \approx 0.30$, and $\nu \approx 4.8$ and (right) $r_1 \approx 1.95$, $r_2 \approx 0.24$, $m \approx 0.72$, and $\nu \approx 3.58$. For the fitted parameter values, we use those in the posterior distribution that yield the minimum distance between the model and the data. To guide the eye, we show simulation results in red between the asterisks and we plot blue lines between the data points. Each frequency plot (bottom panels) represents a random weighted sample (of size 10,000) from the PMC-ABC's posterior distribution of the parameter values at the strictest tolerance level (i.e., $\text{Tol}_{13} \approx 0.0245$ in the left panel and $\text{Tol}_{13} \approx 0.0231$ in the right panel). The squared distances (see Eq. (C.1)) between the asterisks (model) and circles (data) are (left) 0.0043 and (right) 0.0039. For more details on parameter fitting, see Appendix C. The unselective predator group consists of data for *Rimostrombidum lacustris*, and the selective predator group consists of data for *Balanion planctonicum*. (To interpret the references to color in this figure legend, see the electronic version of this article.)

models *phenotypic plasticity*; Kelly et al., 2012) for how rapid adaptation affects population dynamics (Shimada et al., 2010; Yamamichi et al., 2011). (For a recent review on theoretical models of eco-evolutionary feedbacks, see Govaert et al. (2018).) It has been suggested that one should be more likely to expect a stable steady state from models that account for phenotypic plasticity than from those that account for rapid evolution, because plastic genotypes respond faster than nonplastic genotypes to fluctuating environmental conditions (Yamamichi et al., 2011). Our modeling work is consistent with this hypothesis, as the piecewise-smooth system (2.1) converges to a steady state for a large region of phase space (Piltz et al., 2014), but the same steady state is unstable – except for one specific scenario ($a_q = q_2$), at which it is linearly stable but nonhyperbolic – in smooth model II (2.9).

The piecewise-smooth system (2.1) and smooth system I (2.2) produce similar behavior for a sufficiently steep hyperbolic

tangent function that corresponds to a large value of k . However, for small k , smooth system I predicts coexistence at steady-state levels when $a_q < q_2/q_1$. (For a discussion of what we mean by “sufficiently large” k , see our linear stability analysis in Section 2.1; for a comparison between the piecewise-smooth system (2.1) and the Lake Constance data, see Piltz et al., 2014.) Smooth model I (2.2) necessitates the incorporation of a parameter k that influences the system's qualitative behavior, whereas smooth system II (2.9) has the same number of parameters as the piecewise-smooth system (2.1) but includes an additional system variable. It can thus be advantageous to study the piecewise-smooth system, especially if one is considering many species, because it allows one to avoid adding new parameters and/or variables. The hyperbolic tangent functions in (2.2) and the increased dimensionality of (2.9) both add complications to analytical calculations and parameter fitting. On the bright side, there are many more standard

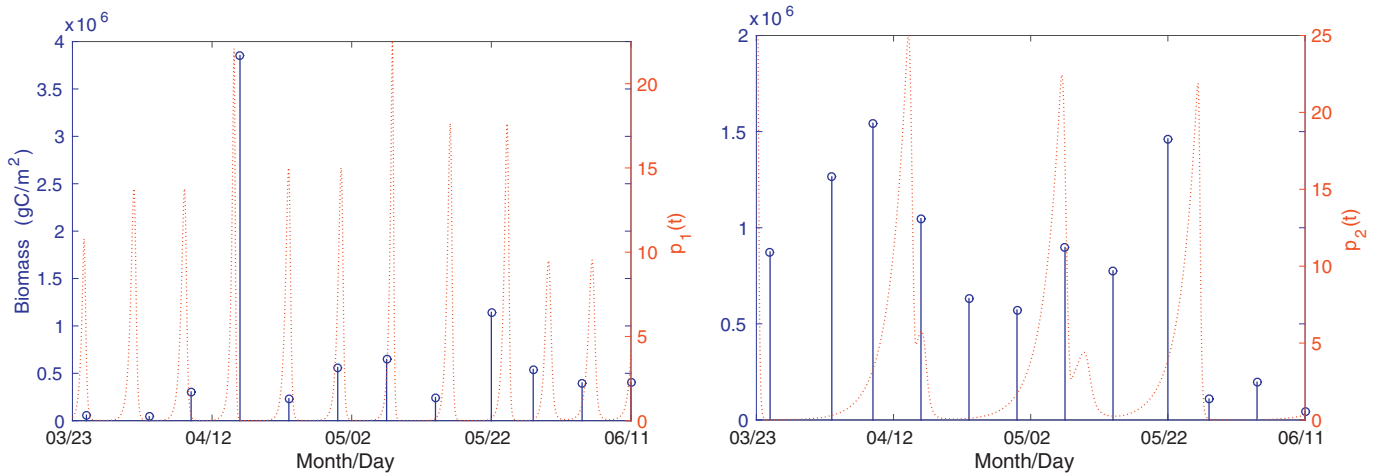


Fig. 6. (Left, red) Preferred-prey abundance $p_1(t)$ and (right, red) alternative-prey abundance $p_2(t)$ for simulations of smooth model II (2.9) using the same parameter values as in the right panel of Fig. 4. We also show (left, circles) preferred and (right, circles) alternative prey data in spring in Lake Constance in 1991. The preferred prey group consists of data for *Cryptomonas ovata*, *Cryptomonas marssonii*, *Cryptomonas reflexa*, *Cryptomonas erosa*, *Rhodomonas lens*, and *Rhodomonas minuta*. The alternative prey group consists of data for small and medium-sized *Chlamydomonas* spp. and *Stephanodiscus parvus*. (To interpret the references to color in this figure legend, see the electronic version of this article.)

numerical techniques and more theory both to determine the stability of steady states and to study bifurcations for smooth dynamical systems than there are for piecewise-smooth ones. One needs to use more involved methods for theory and numerical computations for piecewise-smooth dynamical systems, and development of these techniques is an active area of research (di Bernardo et al., 2008). However, one can derive an analytical expression (using the equation $h = \beta_1 p_1 - a_q \beta_2 p_2 = 0$) for the flow at the discontinuity boundary of (2.1), and the available theory for piecewise-smooth dynamical systems identifies the bifurcation that takes place in (2.1) as a_q crosses the value $a_q = q_2/q_1$ (Piltz et al., 2014). These results help facilitate understanding of the behavior of (2.1), and they are useful for analyzing the ciliate–algae dynamics that are predicted by this piecewise-smooth model (Piltz et al., 2014).

Both of our smooth models successfully reproduce the peak population densities and suggest a parameter regime – when $a_q < q_2/q_1$ for smooth model I (2.2) and for a large perturbation from the coexistence steady state for smooth model II (2.9) – that fits the data for ciliate predators in Lake Constance in the springs of 1991 and 1998. (Note that our initial distributions for these parameters in the fitting algorithm include both parameter regimes in which the coexistence steady state is stable and ones in which it is unstable.) Additionally, when using the parameters that we obtain from fitting smooth model II to data for the unselective predator in 1991, we observe agreement between our model’s output and both (i) the periodicity of the peak preferred-prey abundances and (ii) the timing of large alternative-prey abundances. Both of our smooth models produce a higher frequency of peak densities than what we observe in the available data. A large period in population oscillations is possible for small organisms, such as plankton, with short lifespans and large population densities. Making measurements more frequently would be a good way to try to validate or refute the periodicity of our smooth models. Additionally, using comparisons with data to help choose between different models is an effective way to increase understanding of the use of a piecewise-smooth model as a simplification when there is a steep transition in plankton-feeding behavior. More generally, such comparisons are also valuable in numerous applications. In practice, one can carry out such a model comparison by implementing algorithms for model-based statistical inference (e.g., approximate Bayesian computation, as in the present paper) (Toni et al., 2009)

or by using existing toolboxes for system identification (e.g., the ones implemented in MATLAB (The MathWorks, Inc., 2014)).

One can further investigate model predictions for trait dynamics and compare them to results from controlled laboratory experiments by considering genetically diverse prey and/or predator populations in which one records the dynamics of the genetic diversity. Parameter fitting to Lake Constance data suggests that the best fit occurs in a parameter regime in which the predator-trait dynamics oscillate abruptly between the maximum and minimum values. In a study of two plankton predators and their evolving algal prey, Hiltunen et al. (2014) showed computationally (and discussed experimental evidence) that there are periods of dominance of one predator followed by a rapid switch to dominance by the other. In Hiltunen et al. (2014), the switch in predator dominance arose from interactions between changes in the predator populations and changes in the frequency of a prey type that develops a predator defense mechanism against one of the two predators. Motivated by the above findings, it is also interesting to consider a model that incorporates a time-scale difference between demographic and predator-trait dynamics (Piltz et al., 2017).

5. Conclusions

To increase biological insight into the experimentally-observed adaptive feeding behavior of unselective and selective ciliate predators on two different types of prey, we constructed two ordinary-differential-equation models for prey switching. In one model (“smooth model I”), we represented the transition from one diet to another using a hyperbolic tangent function; in the other (“smooth model II”), we added a new system variable to describe the diet switch in the system (and we hence increased the system’s dimensionality by 1). In constructing these models, we relaxed the simplifying assumption of a “discontinuous” predator feeding behavior in a piecewise-smooth dynamical system that a subset of us used previously to suggest prey switching as a possible mechanistic explanation for the observed dynamics (Piltz et al., 2014). Based on our results from fitting parameters of the two smooth systems to data on freshwater plankton, we conclude that the best fit to the data occurs when prey switching is rapid (and hence steep in the continuous models) and that the simplifying assumption of discontinuous predator feeding behavior appears to be justified.

Similar to earlier investigations, such as those by Jeffrey (2011) and Leifeld et al. (2015), our study provides an illustrative example of both similarities and differences between a discontinuous system and smooth regularizations of it. When piecewise-smooth dynamical systems are used to simplify transitions in applications – such as approximating a cubic function in a membrane potential in models of spiking neurons (McKean, 1970), Hill functions in models of genetic regulatory networks (Glass, 1975), changes in the Earth’s reflectivity due to ice melt in climate models (Abbot et al., 2011), and more – understanding the extent to which the behavior of corresponding smooth and piecewise-smooth systems agree is crucial for generating both accurate model simplifications and accurate predictions.

Finally, using the data that we currently possess, it is difficult to determine which of the three models (i.e., a piecewise-smooth model and the two smooth systems with an adaptive predator) provides a better mechanistic explanation for the observations of ciliate–algae dynamics in spring in Lake Constance. To enhance model selection, it would be very useful to collect data to improve analysis of the steepness of prey switching, the functional form of the preference tradeoff, and the periodicity of the population oscillations. Nevertheless, the construction of models using alternative mathematical frameworks, examining the relationships between them, and comparing them to data can greatly increase understanding of the underlying mechanisms in biological systems.

Acknowledgements

We thank John Hogan, Philip Maybank, Frank Schilder, and Frits Veerman for helpful discussions. We thank Ursula Gaedke for sending us the Lake Constance data, which were obtained as part of the Collaborative Programme SFB 248 funded by the German Science Foundation. SHP was supported by the Osk. Hutunnen Foundation (OHF) and the Engineering and Physical Sciences Research Council (EPSRC) through the Oxford Life Sciences Interface Doctoral Training Centre and by the People Programme (Marie Curie Actions) of the European Union’s Seventh Framework Programme (FP7/2007–2013) under REA grant agreement #609405 (COFUNDPostdocDTU). PKM would like to thank the Mathematical Biosciences Institute (MBI) at The Ohio State University for partially supporting this research. MBI receives its funding through National Science Foundation grant DMS1440386. We thank the anonymous referees for helpful comments.

Appendix A. Stability of the coexistence steady state in smooth model I

In this appendix, we prove Propositions 2.1 and 2.2.

Proof. The Jacobian for Eq. (2.2) is

$$\begin{bmatrix} r_1 - \frac{z}{2}B(1 + p_1kC) & \frac{zp_1ka_q}{2}BC & -\frac{p_1}{2}B \\ \frac{zp_2k}{2}BC & r_2 - \frac{z}{2}C(1 + p_2ka_qB) & -\frac{p_2}{2}C \\ \frac{eq_1z}{2}B(1 + p_1kC) - \frac{eq_2p_2zk}{2}BC & \frac{eq_2z}{2}C(1 + p_2ka_qB) - \frac{eq_1p_1zka_q}{2}BC & \frac{eq_1p_1}{2}B + \frac{eq_2p_2}{2}C - m \end{bmatrix}, \tag{A.1}$$

where

$$\begin{aligned} A &= \tanh(k(p_1 - a_qp_2)), \\ B &= 1 + A, \\ C &= 1 - A. \end{aligned} \tag{A.2}$$

At the coexistence steady state (2.7), the Jacobian (A.1) is

$$\frac{1}{r_1 + r_2} \begin{bmatrix} -2r_1r_2k\tilde{p}_1 & 2r_1r_2ka_q\tilde{p}_1 & -r_1\tilde{p}_1 \\ 2r_1r_2k\tilde{p}_2 & -2r_1r_2ka_q\tilde{p}_2 & -r_2\tilde{p}_2 \\ eq_1r_1(r_1 + r_2) + 2er_1r_2k(q_1\tilde{p}_1 - q_2\tilde{p}_2) & eq_2r_2(r_1 + r_2) + 2er_1r_2ka_q(q_2\tilde{p}_2 - q_1\tilde{p}_1) & 0 \end{bmatrix}, \tag{A.3}$$

which we henceforth denote by J for the rest of the present appendix. The characteristic polynomial of (A.3) is

$$\det(\lambda I - J) = \lambda^3 + a\lambda^2 + b\lambda + c, \tag{A.4}$$

where

$$\begin{aligned} a &= \frac{2k(p_1 + a_qp_2)r_1r_2}{r_1 + r_2}, \\ b &= \frac{1}{(r_1 + r_2)^2} e(2kp_1^2q_1r_1^2r_2 + p_2q_2r_2^2(r_1 + 2a_qkp_2r_1 + r_2) \\ &\quad + p_1r_1(-2kp_2q_2r_1r_2 + q_1(r_1^2 + r_1r_2 - 2a_qkp_2r_2^2))), \\ c &= \frac{2ekp_1p_2r_1r_2(a_qq_1r_1 + q_2r_2)}{r_1 + r_2}. \end{aligned} \tag{A.5}$$

By the Routh–Hurwitz criterion (Hurwitz, 1895; Routh, 1877), the coexistence steady state (2.7) is asymptotically stable if and only if the coefficients in (A.5) satisfy $a > 0$, $c > 0$, and $ab - c > 0$. The conditions $a > 0$ and $c > 0$ are satisfied because of the positivity of the system parameters. To study the third condition, we write $ab - c$ as a polynomial in k . We thereby obtain

$$ab - c = \frac{2r_1r_2}{e(a_qq_1r_1 + q_2r_2)^2(r_1 + r_2)^2} (p_1r_1 - a_qp_2r_2)s(k),$$

where

$$s(k) = s_2k^2 + s_1k + s_0, \tag{A.6}$$

with

$$\begin{aligned} s_0 &= \frac{1}{2}e^2q_1q_2r_1r_2 \log\left(\frac{r_1}{r_2}\right) \\ &\quad \times \left[2a_qq_1r_1 + 2q_2r_2 + (-a_qq_1r_1 + q_2r_2) \log\left(\frac{r_1}{r_2}\right) \right], \\ s_1 &= em \left[(r_1 + r_2)(a_q^2q_1^2r_1^2 - q_2^2r_2^2) - r_1r_2(a_q^2q_1^2r_1 + q_2^2r_2 \right. \\ &\quad \left. - 3a_qq_1q_2(r_1 + r_2)) \log\left(\frac{r_1}{r_2}\right) \right], \\ s_2 &= 4a_qm^2(a_qq_1 - q_2)r_1r_2(r_1 + r_2). \end{aligned}$$

Using the steady state (2.7), we see that

$$p_1r_1 - a_qp_2r_2 = \frac{a_qkm(r_1^2 - r_2^2) + e(a_qq_1 + q_2)r_1r_2 \arctanh\left(\frac{r_1 - r_2}{r_1 + r_2}\right)}{ek(a_qq_1r_1 + q_2r_2)} > e0.$$

We have thus established that $ab - c > 0 \Leftrightarrow s(k) > 0$.

The value of s at $k = k_0$ in Eq. (2.8) is positive:

$$s(k_0) = \frac{e^2q_1r_1(a_qq_1r_1 + q_2r_2)^2 \log\left(\frac{r_1}{r_2}\right) \left[r_1 + r_2 + r_2 \log\left(\frac{r_1}{r_2}\right) \right]}{2(r_1 + r_2)} > 0. \tag{A.7}$$

For $a_q \geq q_2/q_1$, the function $s(k)$ is concave up with a positive derivative at k_0 , because

$$s'(k_0) = em(a_q q_1 r_1 + q_2 r_2) \times \left[(r_1 + r_2)(a_q q_1 r_1 - q_2 r_2) + (3a_q q_1 - q_2)r_1 r_2 \log\left(\frac{r_1}{r_2}\right) \right] > 0. \tag{A.8}$$

Therefore, $a_q \geq q_2/q_1$ implies that $s(k) > 0$ for all $k > k_0$. Finally, if $a_q < q_2/q_1$, we see that $s(k)$ is a downward-opening parabola. Because $s(k_0) > 0$, it follows that $s(k)$ is positive for $k \in (k_0, k_1)$, where

$$k_1 = \frac{-s_1 + \sqrt{s_1^2 - 4s_2 s_0}}{2s_2}. \tag{A.9}$$

□

Appendix B. Stability of the coexistence steady state in smooth model II

In this appendix, we prove Propositions 2.3 and 2.4. Both proofs use the characteristic polynomial of the Jacobian of smooth system II (2.9). This Jacobian is

$$J = \begin{pmatrix} r_1 - \tilde{q}\tilde{z} & 0 & -\tilde{q}\tilde{p}_1 & -\tilde{p}_1\tilde{z} \\ 0 & r_2 - (1 - \tilde{q})\tilde{z} & -(1 - \tilde{q})\tilde{p}_2 & \tilde{p}_2\tilde{z} \\ e\tilde{q}\tilde{z} & e(1 - \tilde{q})q_2\tilde{z} & e\tilde{q}\tilde{p}_1 + e(1 - \tilde{q})q_2\tilde{p}_2 - m & e\tilde{p}_1\tilde{z} - eq_2\tilde{p}_2\tilde{z} \\ \tilde{q}(1 - \tilde{q}) & -a_q\tilde{q}(1 - \tilde{q}) & 0 & (1 - 2\tilde{q})(\tilde{p}_1 - a_q\tilde{p}_2) \end{pmatrix}. \tag{B.1}$$

At the coexistence steady state (2.10), the Jacobian (B.1) is

$$J = \begin{pmatrix} 0 & 0 & \frac{-r_1 a_q m}{e(r_1 a_q + r_2 q_2)} & \frac{-a_q m(r_1 + r_2)^2}{e(r_1 a_q + r_2 q_2)} \\ 0 & 0 & \frac{-r_2 m}{e(r_1 a_q + r_2 q_2)} & \frac{m(r_1 + r_2)^2}{e(r_1 a_q + r_2 q_2)} \\ er_1 & er_2 q_2 & 0 & \frac{e(a_q - q_2)m(r_1 + r_2)^2}{e(r_1 a_q + r_2 q_2)} \\ \frac{r_1 r_2}{(r_1 + r_2)^2} & \frac{-a_q r_1 r_2}{(r_1 + r_2)^2} & 0 & 0 \end{pmatrix}, \tag{B.2}$$

whose eigenvalues are given by the roots of the characteristic polynomial

$$\det(\lambda I - J) = \lambda^4 + \frac{m(eq_2 r_2^2 + a_q r_1 (er_1 + 2r_2))}{e(a_q r_1 + q_2 r_2)} \lambda^2 + \frac{a_q r_1 r_2 m^2 (a_q - q_2) (r_1 - r_2)}{e(a_q r_1 + q_2 r_2)^2} \lambda + \frac{a_q r_1 r_2 m^2 (r_1 + r_2)}{e(a_q r_1 + q_2 r_2)}. \tag{B.3}$$

Proof. (Proposition 2.3)

For $a_q = q_2$, the $\mathcal{O}(\lambda)$ term in Eq. (B.3) vanishes. Substituting $u = \lambda^2$ yields

$$u^2 + \frac{m[2r_1 r_2 + e(r_1^2 + r_2^2)]}{e(r_1 + r_2)} u + \frac{m^2 r_1 r_2}{e}. \tag{B.4}$$

One can write the discriminant of (B.4) as

$$D = \frac{m^2}{e^2 (r_1 + r_2)^2} \left((r_1^2 + r_2^2)^2 \left(e - \frac{4r_1^2 r_2^2}{(r_1^2 + r_2^2)^2} \right)^2 + \frac{4r_1^2 r_2^2 (r_1^2 - r_2^2)^2}{(r_1^2 + r_2^2)^2} \right). \tag{B.5}$$

Note that D is always positive, so the two roots (u_1 and u_2) of (B.4) are both real. Furthermore, because the polynomial (B.4) is increasing and positive at the intersection of (B.4) with the vertical axis, the roots of the polynomial (B.4) are both negative. Consequently, the four eigenvalues λ_j (with $j \in \{1, 2, 3, 4\}$) consist of two complex-conjugate pairs with 0 real part: $\lambda_{1,2} = \pm\sqrt{-u_1}i$ and $\lambda_{3,4} = \pm\sqrt{-u_2}i$. We thus see that all eigenvalues are purely imaginary. □

Proof. (Proposition 2.4)

First, we prove by contradiction that there is at least one eigenvalue with a nonzero real part. Assume that all four eigenvalues are purely imaginary. One can then write the characteristic polynomial (B.3) as

$$\chi(\lambda) = \prod_{j=1}^4 (\lambda - iy_j), \quad y_j \in \mathbb{R}. \tag{B.6}$$

Expanding χ , we see that the $\mathcal{O}(\lambda)$ coefficient is

$$i(y_1 y_2 y_3 + y_1 y_2 y_4 + y_1 y_3 y_4 + y_2 y_3 y_4),$$

which is purely imaginary. However, (B.3) has a real coefficient for $\mathcal{O}(\lambda)$ that is nonzero for $a_q \neq q_2$. Therefore, there exists at least one eigenvalue with a nonzero real part.

To complete the proof, we show that there are two eigenvalues whose real parts have opposite signs. We denote the roots of (B.3) by λ_j (with $j \in \{1, 2, 3, 4\}$), and we order the roots so that the real part of λ_1 is nonzero. Because $\sum_{j=1}^4 \lambda_j = \text{Tr}(J) = 0$, at least one of λ_2, λ_3 , or λ_4 must have a real part whose sign is opposite to that of λ_1 . Consequently, the steady state is unstable. □

Appendix C. Parameter fitting

We perform parameter fitting using Bayesian inference. In contrast to least-squares fitting, this allows one to study the results from the posterior parameter distribution, rather than just from a single value that gives the best fit as a result of an optimization method. We fit parameters to data with approximate Bayesian computation (ABC) combined with a population Monte Carlo (PMC) method.⁵ See p. 987 of Beaumont et al. (2009).

C1. Smooth model I

Let $z(t; r_1, r_2, m, a_q, k)$ denote the solution of (2.2) with initial values $(p_1(0), p_2(0), z(0)) = (1, 1, 1)$, and let \mathbf{z} denote the available measurement data for the predator population. The data were measured at time instances t_i , so – without measurement errors – the data would be $z_i = z(t_i; r_1, r_2, m, a_q, k)$ for some unknown, true parameter values. We account for the presence of measurement errors by incorporating normally-distributed noise into the results of our model simulations. Specifically, for given parameter values $(\sigma, r_1, r_2, m, a_q, k)$, the model prediction \mathbf{z}^* is described element-wise as $z_i^* \sim \mathcal{N}(z(t_i; r_1, r_2, m, a_q, k), \sigma^2(1 + P_{*,\max})^2)$, where $P_{*,\max}$ is the maximum predator density in a model trajectory. We compute a model trajectory by simulating the model for about 400 days and discarding the first approximately 60 days (corresponding to the two winter months January and February) as a transient. We then align the peak abundances in the data and in the model trajectory that we obtain by simulating the model with the given parameter values. One can construe this procedure as introducing a phase shift in the model results before calculating the distance between the model output and the data.⁶ Because we do not know the variance of measurement errors in advance,

⁵ Before using our implementation of the PMC-ABC algorithm to fit the parameters of our models, we verified our implementation by (i) reproducing results in Beaumont et al. (2009) and (ii) inferring parameters of a Lotka-Volterra system with simulated (and noisy) data.

⁶ Such a procedure results in several candidate parameter sets that need to be rejected (e.g., because they yield a steady state); this increases computation time. An alternative to using a phase shift is to fit the initial values simultaneously with the model parameters. In such an approach, one can compare the distances between the periodic orbits that result from the model to those in the data. However, it is not clear how one should choose a reasonable time window for fitting the initial values and whether such a modification would yield more effective parameter fitting than our current approach.

we incorporate the estimation of σ into our parameter-fitting process.

We assume that the estimated parameters are mutually independent and have known, finite lower and upper bounds. In the employed Bayesian framework, this information is described by independent uniform probability densities. Consequently, we let $\sigma \sim \mathcal{U}(0, 0.1)$, $r_1 \sim \mathcal{U}(1, 3)$, $r_2 \sim \mathcal{U}(0.01, 0.8)$, $m \sim \mathcal{U}(0.1, 1)$, $a_q \sim \mathcal{U}(0.01, 2)$, and $k \sim \mathcal{U}(1, 100)$. We choose these lower and upper bounds based on studying the literature (see, for example, Tirok and Gaedke, 2010), simulating smooth systems I and II numerically, and testing our implementation of the PMC-ABC method with several different uniform priors. Because of the independence of the parameters, one can express the joint prior as the product of the probability density functions of the parameters.

As a measure of discrepancy, we use the Euclidean distance between normalized data and model trajectories. We calculate

$$d(\mathbf{z}^*, \mathbf{z}) = \frac{1}{N} \left| \frac{\mathbf{z}^*}{|\mathbf{z}^*|} - \frac{\mathbf{z}}{|\mathbf{z}|} \right|^2. \quad (\text{C.1})$$

We determine a decreasing sequence of tolerance thresholds by setting the threshold of the subsequent iteration to be either (i) the largest distance between the data and the model output of the best 10% quantile of the current step or (ii) equal to the tolerance threshold of the current step (if the distance using the 10% quantile is larger than the current tolerance threshold). Based on several test runs, we choose the following initial tolerance levels. For smooth model I (2.2), we choose an initial tolerance of $\text{ToI}_1 \approx 0.022$ for a selective predator in 1991, $\text{ToI}_1 \approx 0.038$ for an unselective predator in 1991, $\text{ToI}_1 \approx 0.0525$ for a selective predator in 1998, and $\text{ToI}_1 \approx 0.0475$ for an unselective predator in 1998.

Finally, to obtain an approximation of the posterior, we iterate the PMC-ABC algorithm 10–15 times to collect 2000 candidate parameters (i.e., values for σ , r_1 , r_2 , m , a_q , and k) at each iteration that yield a distance between the perturbed model output and the data that is smaller than a given tolerance threshold. (Before computing the distance, if a candidate set of parameters is not in the domain of the prior, we reject the candidate and draw a new sample.) We indicate the final tolerances in the figure captions.

C2. Smooth model II

Our parameter-fitting procedure for smooth model II deviates only slightly from the process that we described in Appendix C.1. We now assume that $m \sim \mathcal{U}(0.05, 1)$ and $\nu \sim \mathcal{U}(1.1, 5)$. The parameter ν represents a perturbation of the predator population from the coexistence steady state, so we simulate smooth model II with $(p_1(0), p_2(0), z(0), q(0)) = (a_q m(r_1 + r_2)/[e(r_1 a_q + r_2 q_2)], m(r_1 + r_2)/[e(r_1 a_q + r_2 q_2)], \nu(r_1 + r_2), r_1/(r_1 + r_2))$ as the initial value. We also omit the parameter a_q , because it is fixed at $a_q = q_2 = 0.5$. We choose the tolerance thresholds using an analogous procedure as the one that we described in Appendix C.1. Our tolerance values are $\text{ToI}_1 \approx 0.02$ for a selective predator in 1991, $\text{ToI}_1 \approx 0.03$ for an unselective predator in 1991, $\text{ToI}_1 \approx 0.0375$ for a selective predator in 1998, and $\text{ToI}_1 \approx 0.032$ for an unselective predator in 1998.

References

- Abbot, D.S., Voigt, A., Koll, D., 2011. The Jormungand global climate state and implications for Neoproterozoic glaciations. *J. Geophys. Res.: Atmos.* 116, D18103. <https://agupubs.onlinelibrary.wiley.com/doi/abs/10.1029/2011JD015927>.
- Abrams, P.A., Matsuda, H., 2003. Population dynamical consequences of reduced predator switching at low total prey densities. *Popul. Ecol.* 45, 175–185.
- Beaumont, M.A., Cornuet, J.-M., Marin, J.-M., Robert, C.P., 2009. Adaptive approximate Bayesian computation. *Biometrika* 96, 983–990.
- di Bernardo, M., Budd, C.J., Champneys, A.R., Kowalczyk, P., 2008. *Piecewise-Smooth Dynamical Systems*. Springer-Verlag. <https://www.springer.com/gp/book/9781846280399>.
- di Bernardo, M., Johansson, K.H., Vasca, F., 2001. Self-oscillations and sliding in relay feedback systems: symmetry and bifurcations. *Int. J. Bifurcation Chaos* 11, 1121–1140. <https://www.worldscientific.com/doi/abs/10.1142/S0218127401002584>.
- Boukal, D.S., Krivan, V., 1999. Lyapunov functions for Lotka–Volterra predator–prey models with optimal foraging behavior. *J. Math. Biol.* 39, 493–517.
- Casey, R., De Jong, H., Gouzé, J.-L., 2006. Piecewise-linear models of genetic regulatory networks: equilibria and their stability. *J. Math. Biol.* 52, 27–56.
- Champneys, A.R., di Bernardo, M., 2008. Piecewise smooth dynamical systems. *Scholarpedia* 3, 4041. http://www.scholarpedia.org/article/Piecewise_smooth_dynamical_systems. Accessed: 12-06-2017.
- Colombo, A., di Bernardo, M., Hogan, S.J., Jeffrey, M.R., 2012. Bifurcations of piecewise smooth flows: perspectives, methodologies and open problems. *Physica D* 241, 1845–1860.
- Dankowicz, H., 2007. On the purposeful coarsening of smooth vector fields. *Nonlinear Dyn.* 50, 511–522.
- Fussmann, G.F., Loreau, M., Abrams, P.A., 2007. Eco-evolutionary dynamics of communities and ecosystems. *Funct. Ecol.* 21, 465–477.
- Gause, G.F., Smaragdova, N.P., Witt, A.A., 1936. Further studies of interaction between predators and prey. *J. Anim. Ecol.* 5, 1–18.
- Glass, L., 1975. Classification of biological networks by their qualitative dynamics. *J. Theor. Biol.* 54, 85–107.
- Govaert, L., Fronhofer, E. A., Lion, S., Eizaguirre, C., Bonte, D., Egas, M., Hendry, A. P., Martins, A. D. B., Melián, C. J., Raeymaekers, J. A. M., Ratikainen, I. I., Saether, B.-E., Schweitzer, J. A., Matthews, B., 2018. Eco-evolutionary feedbacks – theoretical models and perspectives. [arXiv:1806.07633](https://arxiv.org/abs/1806.07633).
- Hiltunen, T., Ellner, S.P., Hooker, G., Jones, L.E., Hairston Jr, N.G., 2014. Eco-evolutionary dynamics in a three-species food web with intraguild predation: intriguingly complex. *Adv. Ecol. Res.* 50, 41–74. <https://www.dora.lib4ri.ch/eawag/islandora/object/eawag:11644>.
- Hinch, E.J., 1991. *Perturbation Methods*. Cambridge University Press. <https://www.cambridge.org/core/books/perturbation-methods/78E3D7607E441E4BCAE84698DE91D3BC>.
- Hogan, S.J., 1989. On the dynamics of rigid-block motion under harmonic forcing. *Proc. R. Soc. Lond. A: Math. Phys. Eng. Sci.* 425, 441–476.
- Hogan, S.J., 2004. The effect of smoothing on bifurcation and chaos computations in non-smooth mechanics. In: *Proceedings of the XXI International Congress of Theoretical and Applied Mechanics*, Warsaw, Poland.
- Holling, C.S., 1965. The functional response of predators to prey density and its role in mimicry and population regulation. *Mem. Entomol. Soc. Can.* 97, 5–60.
- Hurwitz, A., 1895. Ueber die Bedingungen, unter welchen eine Gleichung nur Wurzeln mit negativen reellen Theilen besitzt. *Mathematische Annalen* 273–284.
- Jeffrey, M.R., 2011. Nondeterminism in the limit of nonsmooth dynamics. *Phys. Rev. Lett.* 106, 254103.
- Jeffrey, M.R., 2014. Hidden dynamics in models of discontinuity and switching. *Physica D* 273–274, 34–45.
- Jeffrey, M.R., 2016. Hidden degeneracies in piecewise smooth dynamical systems. *Int. J. Bifurcation Chaos* 26, 1650087.
- Jeffrey, M.R., 2016. Smoothing tautologies, hidden dynamics, and sigmoid asymptotics in piecewise smooth systems. *Chaos* 25, 103125. <https://aip.scitation.org/doi/abs/10.1063/1.4934204>.
- Jones, C.K.R.T., 1994. Geometric singular perturbation theory. In: Arnold, L. (Ed.), *Dynamical systems, Lecture Notes in Mathematics*, vol. 1609. Springer-Verlag, pp. 44–118. <https://link.springer.com/chapter/10.1007/BFb0095239>
- Kelly, S.A., Panhuis, T.M., Stoehr, A.M., 2012. Phenotypic plasticity: molecular mechanisms and adaptive significance. *Compr. Physiol.* 2, 1417–1439. <https://onlinelibrary.wiley.com/doi/abs/10.1002/cphy.c110008>.
- Křivan, V., 1996. Optimal foraging and predator–prey dynamics I. *Theor. Popul. Biol.* 49, 265–290.
- Kruschke, J.K., 2013. Bayesian estimation supersedes the *t* test. *J. Exp. Psychol.: General* 142, 573–603.
- Kuehn, C., 2015. *Multiple Time Scale Dynamics*. Springer-Verlag. <https://www.springer.com/gp/book/9783319123158>.
- Křivan, V., Eissner, J., 2003. Optimal foraging and predator–prey dynamics, III. *Theor. Popul. Biol.* 63, 269–279.
- Křivan, V., 2007. The Lotka–Volterra predator–prey model with foraging–predation risk trade-offs. *Am. Nat.* 170, 771–782.
- Křivan, V., SIKDER, A., 1999. Optimal foraging and predator–prey dynamics II. *Theor. Popul. Biol.* 55, 111–126.
- van Leeuwen, E., Brännström, Å., Jansen, V.A.A., Dieckmann, U., Rossberg, A.G., 2013. A generalized functional response for predators that switch between multiple prey species. *J. Theor. Biol.* 328, 89–98.
- van Leeuwen, E., Jansen, V.A.A., Bright, P.W., 2007. How population dynamics shape the functional response in a one-predator–two-prey system. *Ecology* 88, 1571–1581. https://www.jstor.org/stable/27651263?seq=1#metadata_info_tab_contents.
- Leifeld, J., Hill, K., Roberts, A., 2015. Persistence of saddle behavior in the nonsmooth limit of smooth dynamical systems. [arXiv:1504.04671](https://arxiv.org/abs/1504.04671).
- McKean, H.P., 1970. Nagumo’s equation. *Adv. Math.* 4, 209–223.
- Müller, H., Schlegel, A., 1999. Responses of three freshwater planktonic ciliates with different feeding modes to cryptophyte and diatom prey. *Aquat. Microb. Ecol.* 17, 49–60.
- Murdoch, W.W., 1969. Switching in general predators: experiments on prey specificity and stability of prey populations. *Ecol. Monogr.* 39, 335–354.
- Piltz, S.H., Porter, M.A., Maini, P.K., 2014. Prey switching with a linear preference trade-off. *SIAM J. Appl. Dyn. Syst.* 13, 658–682.

- Piltz, S.H., Veerman, F., Maini, P.K., Porter, M.A., 2017. A predator–2 prey fast–slow dynamical system for rapid predator evolution. *SIAM J. Appl. Dyn. Syst.* 16, 54–90.
- Post, D.M., Connors, M.E., Goldberg, D.S., 2000. Prey preference by a top predator and the stability of linked food chains. *Ecology* 81, 8–14.
- Routh, E.J., 1877. *A Treatise on the Stability of a Given State of Motion, Particularly Steady Motion*. Macmillan and Company.
- Shimada, M., Ishii, Y., Shibao, H., 2010. Rapid adaptation: a new dimension for evolutionary perspectives in ecology. *Popul. Ecol.* 52, 5–14.
- Sommer, U., Adrian, R., Domis, L.D.S., Elser, J.J., Gaedke, U., Ibelings, B., Jeppesen, E., Lurling, M., Molinero, J.C., Mooij, W.M., van Donk, E., Winder, M., 2012. Beyond the plankton ecology group (PEG) model: mechanisms driving plankton succession. *Annu. Rev. Ecol. Evol. Syst.* 43, 429–448.
- Sotomayor, J., Teixeira, M.A., 1996. Regularization of discontinuous vector fields. In: *International Conference on Differential Equations, Lisboa, Equadiff 95, 1996*, pp. 207–223. <https://www.worldscientific.com/worldscibooks/10.1142/3746#t=toctoc>.
- Stephens, D.W., Krebs, J.R., 1987. *Foraging Theory*. Princeton University Press. <https://press.princeton.edu/titles/2453.html>
- Stommel, H., 1961. Thermohaline convection with two stable regimes of flow. *Tellus* 13, 224–230. <https://onlinelibrary.wiley.com/doi/abs/10.1111/j.2153-3490.1961.tb00079.x>.
- Teixeira, M.A., da Silva, P.R., 2012. Regularization and singular perturbation techniques for non-smooth systems. *Physica D* 241, 1948–1955.
- The MathWorks, Inc., 2018. Natick, Massachusetts, USA.
- Tirok, K., Gaedke, U., 2006. Spring weather determines the relative importance of ciliates, rotifers and crustaceans for the initiation of the clear-water phase in a large, deep lake. *J. Plankton Res.* 28, 361–373.
- Tirok, K., Gaedke, U., 2007. Regulation of planktonic ciliate dynamics and functional composition during spring in Lake Constance. *Aquat. Microb. Ecol.* 49, 87–100.
- Tirok, K., Gaedke, U., 2007. The effect of irradiance, vertical mixing and temperature on spring phytoplankton dynamics under climate change: long-term observations and model analysis. *Oecologia* 150, 625–642. https://www.jstor.org/stable/40210580?seq=1#metadata_info_tab_contents
- Tirok, K., Gaedke, U., 2010. Internally driven alternation of functional traits in a multispecies predator–prey system. *Ecology* 91, 1748–1762.
- Toni, T., Welch, D., Strelkowa, N., Ipsen, A., Stumpf, M.P.H., 2009. Approximate Bayesian computation scheme for parameter inference and model selection in dynamical systems. *J. R. Soc. Interface* 6, 187–202.
- Verity, P., 1991. Feeding in planktonic protozoans: evidence for nonrandom acquisition of prey. *J. Protozool.* 38, 69–76.
- Yamamichi, M., Yoshida, T., Sasaki, A., 2011. Comparing the effects of rapid evolution and phenotypic plasticity on predator–prey dynamics. *Am. Nat.* 178, 287–304.